

## Anharmonic Thermal Oscillations of the Electron Momentum Distribution in Lithium Fluoride

A. Erba,<sup>1,\*</sup> J. Maul,<sup>1,2</sup> M. Itou,<sup>3</sup> R. Dovesi,<sup>1</sup> and Y. Sakurai<sup>3</sup>

<sup>1</sup>*Dipartimento di Chimica and Centre of Excellence NIS (Nanostructured Interfaces and Surfaces), Università di Torino, via Giuria 5, IT-10125 Torino, Italy*

<sup>2</sup>*Laboratório de Combustíveis e Materiais, INCTMN-UFPB, Universidade Federal da Paraíba, CEP 58051-900, João Pessoa, Paraíba, Brazil*

<sup>3</sup>*Japan Synchrotron Radiation Research Institute, SPring-8 1-1-1 Kouto, Sayo, Hyogo 679-5198 Japan*

(Received 24 April 2015; published 10 September 2015)

Anharmonic thermal effects on the electron momentum distribution of a lithium fluoride single crystal are experimentally measured through high-resolution Compton scattering and theoretically modeled with *ab initio* simulations, beyond the harmonic approximation to the lattice potential, explicitly accounting for thermal expansion. Directional Compton profiles are measured at two different temperatures, 10 and 300 K, with a high momentum space resolution (0.10 a.u. in full width at half maximum), using synchrotron radiation. The effect of temperature on measured directional Compton profiles is clearly revealed by oscillations extending almost up to  $|p| = 4$  a.u., which perfectly match those predicted from quantum-mechanical simulations. The wave-function-based Hartree-Fock method and three classes of the Kohn-Sham density functional theory (local-density, generalized-gradient, and hybrid approximations) are adopted. The lattice thermal expansion, as described with the quasiharmonic approach, is found to entirely account for the effect of temperature on the electron momentum density within the experimental accuracy.

DOI: [10.1103/PhysRevLett.115.117402](https://doi.org/10.1103/PhysRevLett.115.117402)

PACS numbers: 78.70.-g, 31.15.A-, 65.40.-b, 71.15.Mb

The electron momentum density (EMD)  $\pi(\mathbf{p})$  of a material embodies valuable chemical and physical details on its electronic ground state, which are complementary to those accessible through the analysis of the electron charge density (ECD)  $\rho(\mathbf{r})$  [1]. In this respect, high-resolution Compton scattering has proven to constitute an effective technique for probing the electronic structure of solids and liquids [2–4]. In recent years, merits and limitations of several quantum-mechanical methods have been assessed by comparing their predictions with accurate experimental Compton profiles (CP): (i) on the one hand, wave-function-based methods, such as the reference Hartree-Fock (HF) and the perturbative MP2 (explicitly accounting for electron-electron dynamic correlation) ones, were found to satisfactorily describe most features of the EMD; (ii) on the other hand, the popular Kohn-Sham formulation of the density functional theory (DFT) has shown definite discrepancies with the experiment, systematically overestimating the anisotropy of the EMD, which can be traced back to its fundamental inability in satisfying the so-called virial theorem,  $-2\langle T \rangle = \langle V \rangle$  (which in the HF method guarantees the balance between potential  $\langle V \rangle$  and kinetic  $\langle T \rangle$  contributions to the total energy of the system), by underestimating the kinetic energy [5–10].

Temperature affects the electron distribution quite differently in position and momentum spaces [11]. As electrons do follow the respective nuclei almost instantaneously, thermal effects on the ECD must be explicitly taken into account, even at room temperature [12]. Thermal effects on

the EMD, on the contrary, are much subtler; for this reason they have been systematically neglected in most theoretical models (see below for a discussion of the few exceptions in this respect) and, more generally, have been overlooked for a long time. In recent years, however, the enhanced accuracy of modern synchrotron radiation-based Compton scattering measurements has allowed for unambiguously detecting such fine effects. Among other investigations, Compton scattering has thus been fruitfully applied to unveil the temperature dependence of the configurational enthalpy in ice, spin, and magnetic moments of several crystals and shape memory alloys, the electron localization state in  $\text{CeRu}_2\text{Si}_2$  below and above the Kondo temperature, etc. [13–19].

From a theoretical point of view, as thermal effects on the EMD of solids are tiny, rather sophisticated computational approaches combined with a high numerical accuracy are required in order to reveal them with general *ab initio* methods. The only *ab initio* study ever attempted in this respect dates back to 1998 when Dugdale and Jarlborg reported a pioneering DFT study of thermal disorder effects on the CP of Li and Na [20]. By keeping the lattice cell fixed (i.e., without accounting for lattice thermal expansion), they computed a Boltzmann statistical average over atomic configurations as obtained through a Gaussian distribution along harmonic phonon modes and reported a large thermal effect, which resulted in a *broadening* of the CP with increasing temperature. Three high-accuracy Compton scattering experiments were performed later

and were unable to confirm this picture and measured an opposite effect: a *narrowing* of the *CP* upon heating [21–23]. In particular, Sternemann and co-workers, by means of *empirical* temperature-dependent local pseudopotential computations, suggested lattice expansion (i.e., the Fermi momentum  $p_F$  change with temperature) to be the dominant effect on the thermal response of the EMD of several simple metals for  $|p| \leq |p_F|$ . In the case of lithium, where higher momentum components (HMC) to the valence EMD of the system show a nonzero dependence on temperature, the need for an explicit treatment of thermal disorder (by means of Debye-Waller factors, for instance) was invoked for  $|p| > |p_F|$  [22–24].

In this Letter, we report the results of a fully *ab initio* anharmonic theoretical investigation of anisotropic thermal effects on the EMD of solids, by explicitly taking into account lattice thermal expansion. The EMD of the simple LiF single crystal is found to be affected by temperature according to a rather complex pattern, which manifests itself in regular oscillations of directional *CPs* (extending well beyond the Fermi momentum, with HMC contributions up to about  $|p| = 4$  a.u.). Highly accurate directional *CPs* of LiF are measured at 10 and 300 K, which show thermal oscillations that perfectly match the predicted ones. Different quantum-chemical methods are used (the wavefunction-based HF one and several formulations of the DFT), which, despite providing slightly different descriptions of the EMD anisotropy and of the equilibrium volume of LiF, all remarkably result in a coherent description of thermal effects on the EMD.

High-resolution directional *CPs* have been measured at the BL08W beam line at the SPring-8 synchrotron-radiation center in Japan. The sample is a single crystal of LiF with a flat surface normal to the [100] direction. The energy of the incident x-ray beams is 115 keV and the scattering angle of 165 degrees. The momentum resolution is 0.10 a.u. The Compton profiles were corrected for absorption, analyzer, and detector efficiencies, scattering cross section, possible double scattering contributions, and x-ray background. All calculations have been performed with the CRYSTAL14 program [25], with atom-centered Gaussian-type function basis sets of TZVP (for DFT) and DZVP (for HF) quality [26]. Phonon frequencies have been computed at 7 volumes on a supercell containing 16 atoms. *CPs* have been computed as Fourier transforms of the autocorrelation function  $B(r)$ , as convoluted for the experimental resolution function. The T1 tolerance for the truncation of infinite lattice sums is set to a tight value of 20 to ensure the nodal condition of  $B(r)$  [8].

Before considering thermal effects on the EMD of LiF, let us briefly illustrate how different quantum-mechanical methods perform in the description of the EMD anisotropy of the system, which was first experimentally determined by Reed and co-workers [27,28] using  $\gamma$  rays, and by Loupias and Petiau [29] using synchrotron radiation. The

valence directional *CP*  $J_{100}(p)$  is shown in the upper panel of Fig. 1, while the three lower panels report the three main directional *CP* anisotropies [given as a percentage of  $J_{100}(0)$ ] of LiF. Along with the experimental determinations, four theoretical predictions are reported as obtained with the HF method and with three functionals that correspond to three distinct rungs of the well-known “Jacob’s ladder” [30]: a local density approximation one (LDA), a generalized gradient approximation one (PBEsol) and a hybrid one (PBE0), which incorporates 25% of the exact HF exchange into its exchange-correlation potential. All methods nicely reproduce the overall features of the EMD anisotropy in terms of position and amplitude of the oscillations, describing the [100]–[111] anisotropy as the largest and the [110]–[111] as the smallest. It has to be noticed that all DFT-based methods do systematically slightly overestimate the amplitude of the oscillations, thus describing a larger EMD anisotropy. The overall description provided by the reference HF method (that, by definition, neglects the whole electron-electron correlation) turns out to be the most satisfactory (particularly so for the subtle [110]–[111] anisotropy), thus confirming the

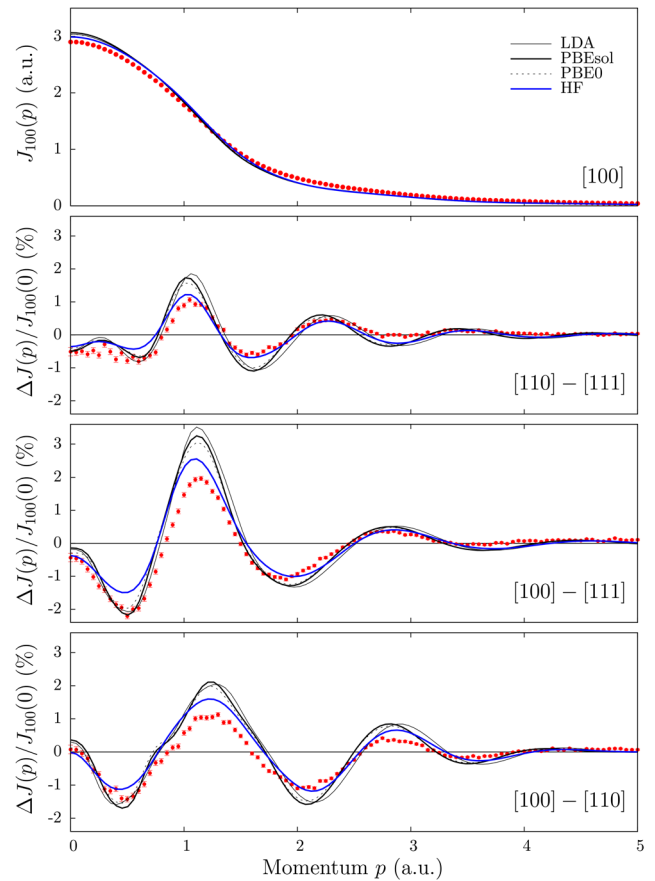


FIG. 1 (color online). (Upper panel) valence  $J_{100}(p)$  *CP* and (lower panels) *CP* anisotropies of single-crystal LiF, as measured (red circles with error bars) and computed (lines) with different quantum-mechanical methods.

importance of satisfying the above-mentioned virial theorem (the  $-2\langle T \rangle / \langle V \rangle$  ratio, that would be 1 in an exact calculation, being 0.999 for HF, 1.055 for LDA, 1.059 for PBEsol, and 1.044 for PBE0).

Within the harmonic approximation to the lattice potential, a variety of solid state thermal properties would be incorrectly described; among others, thermal expansion would be null, elastic constants and bulk modulus would not depend on temperature, thermal conductivity would be infinite as well as phonon lifetimes, etc. [31,32]. A relatively simple, though effective, approach for correcting most of these deficiencies is represented by the so-called quasiharmonic approximation (QHA) [33–35] according to which, the Helmholtz free energy of a crystal is written retaining the same harmonic expression but introducing an explicit dependence of vibration frequencies on volume:

$$F(T, V) = U_0(V) + k_B T \sum_{\mathbf{k}p} \left[ \ln \left( 1 - e^{-\frac{\hbar \omega_{\mathbf{k}p}(V)}{k_B T}} \right) \right], \quad (1)$$

where  $k_B$  is Boltzmann's constant,  $U_0(V)$  is the zero-temperature internal energy of the crystal, which includes the zero-point energy of the system:  $E_0^{ZP}(V) = \sum_{\mathbf{k}p} \hbar \omega_{\mathbf{k}p}(V) / 2$ , and the sum runs over phonons within the first Brillouin zone in reciprocal space. The volumetric thermal expansion coefficient,  $\alpha_V(T) = 1/V(T) [\partial V(T) / \partial T]$ , can then be derived by minimizing Eq. (1) with respect to the volume at each temperature. As LiF is a cubic crystal, the linear thermal expansion coefficient is simply  $\alpha_a = \alpha_V / 3$ . Within the QHA, in order to describe the thermal expansion, just the volume dependence of the lattice free energy of Eq. (1) has to be properly converged; a  $2 \times 2 \times 2$  sampling of the phonon dispersion in the first Brillouin zone of LiF turns out to provide fully converged results, which are shown in Fig. 2. In the upper panel, the lattice parameter  $a$  is reported as a function of temperature, as computed with the four different methods and compared with experimental determinations: (i) the different quantum-mechanical schemes provide rather different absolute values of  $a$  (with differences as large as 2.3% among them); (ii) LDA and HF give the closest descriptions to the experiment; (iii) PBEsol and PBE0 overestimate the lattice parameter by almost the same amount.

Despite the different description of the absolute value of  $a$ , all methods do provide a satisfactory description of its thermal dependence up to room temperature (this being the most important aspect for the correct description of thermal effects on the EMD, as shown below) with slight differences among them. In order to highlight such differences, we report the linear thermal expansion coefficient  $\alpha_a$  of LiF in the lower panel of Fig. 2. As expected from previous investigations [34,35,38,39], the LDA scheme underestimates the thermal expansion. The reference HF method overestimates  $\alpha_a$  whereas the two schemes

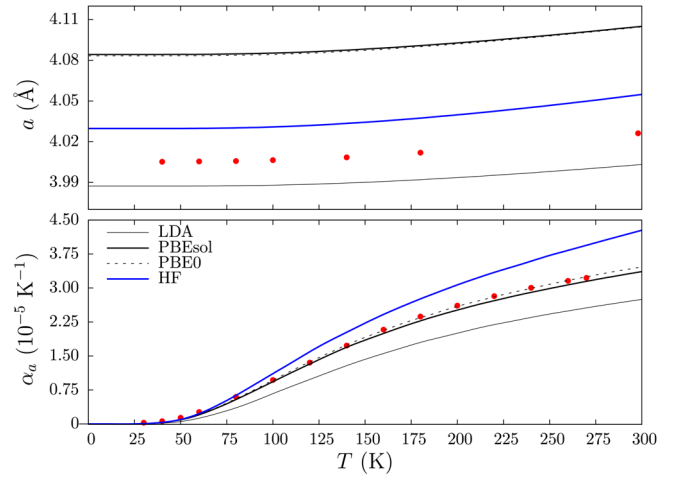


FIG. 2 (color online). Lattice parameter  $a$  (upper panel) and linear thermal expansion coefficient  $\alpha_a$  (lower panel) of LiF, as a function of temperature. Experimental data are from Refs. [36,37].

(PBEsol and PBE0) that provide the poorest description of the absolute value of  $a$ , are found to perfectly predict the thermal expansion of the system.

As the integral of a directional  $CP$   $J(p)$  along the whole electron momentum axis  $p$  is normalized to the number of electrons per cell, it is expected that temperature would manifest itself in regular and damped oscillations of  $J(p)$ . In the upper panel of Fig. 3, we report our experimentally

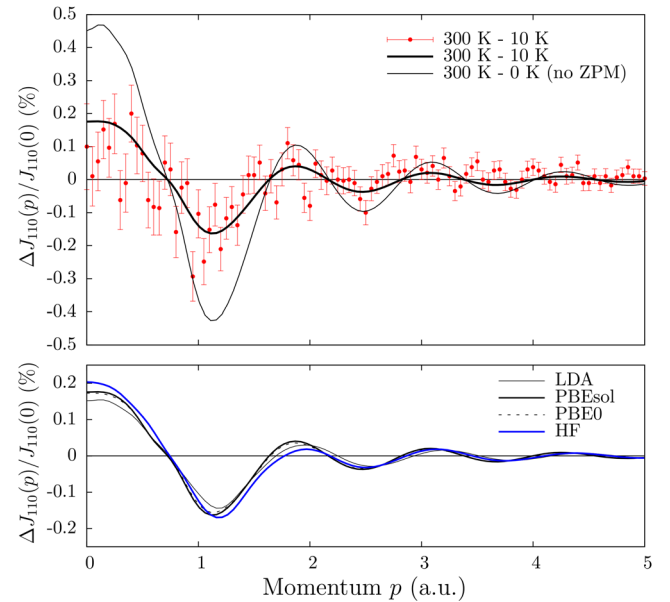


FIG. 3 (color online). Difference of the  $J_{110}(p)$  valence  $CP$  of LiF between 300 and 10 K [given as percentage of  $J_{110}(0)$ ]. In the upper panel, computed PBEsol values (thick line) are compared with measured ones (symbols with error bars); the thin line corresponds to the PBEsol computed difference between 300 and 0 K, without including ZPM effects. In the lower panel, predictions from different theoretical methods are compared.

measured difference of the directional  $J_{110}(p)$  CP of LiF between 300 and 10 K, which shows clear oscillations almost up to  $|p| = 4$  a.u. Previous high-resolution experimental measurements of thermal effects on CPs revealed such oscillations on simple metals: *empirical* calculations supported the picture according to which the large oscillations at small momenta,  $|p| < |p_F|$ , were mainly due to thermal expansion while the small oscillations at higher momenta (when detected) to thermal disorder [22–24]. Along with experimental measurements, the upper panel of Fig. 3 also reports the computed thermal effect on  $J_{110}(p)$ , as obtained by taking into account the thermal expansion of the lattice, with the PBEsol method including zero-point motion (thick line). The agreement with the experimental determinations is extremely remarkable (in terms of position and amplitude of the oscillations), both at low and high momenta, and it demonstrates that an accurate *ab initio* description of lattice thermal expansion can account for the whole thermal effect on the EMD of LiF, within the experimental accuracy. A couple of further considerations: (i) the effect of an increasing temperature is clearly that of *narrowing* the CP; (ii) zero-point motion (ZPM), often neglected in most computational studies, has a large effect and must be explicitly considered in order to predict the correct amplitude of thermal oscillations on the EMD (see thin line in the upper panel of the figure); (iii) different quantum-mechanical methods do provide a rather similar and homogeneous description of thermal effects on the EMD of the system (see the lower panel of the figure), suggesting that such thermal effects are dominated by the

description of thermal expansion, rather than by the agreement with absolute values of the equilibrium volume at different temperatures.

A deeper insight on how thermal lattice expansion is affecting the electronic properties of LiF in momentum space can be achieved by directly looking at the computed EMD  $\pi(p)$  [40]. In Fig. 4, we report the PBE0 valence EMD of the system as mapped in the (100) and (110) planes (upper panels), along with the two corresponding thermal differences between 300 and 10 K (lower panels). Temperature is seen to affect the EMD according to rather complex and definitely anisotropic patterns, which show a region at small momenta,  $|p| \lesssim |p_F|$ , where the EMD overall increases and another region at higher momenta,  $|p| \approx |1.3|$  a.u., where it decreases. Above  $|p| = 1.5$  a.u., the EMD of LiF appears to be scarcely affected by temperature.

To summarize, in this Letter we have shown how anharmonic thermal effects on the EMD of solids can reliably and quantitatively be predicted by highly accurate *ab initio* quantum-mechanical simulations, accounting for thermal expansion effects. Thermal oscillations of CPs of LiF, as measured by high-resolution Compton scattering, are nicely reproduced by the theory both at low and high momenta.

J. M. acknowledges the Brazilian scholarship program “Ciência sem Fronteiras” (Process No. 248425/2013-7/SWE). The Compton scattering experiment was performed with the approval of JASRI (Proposal No. 2009A2022).

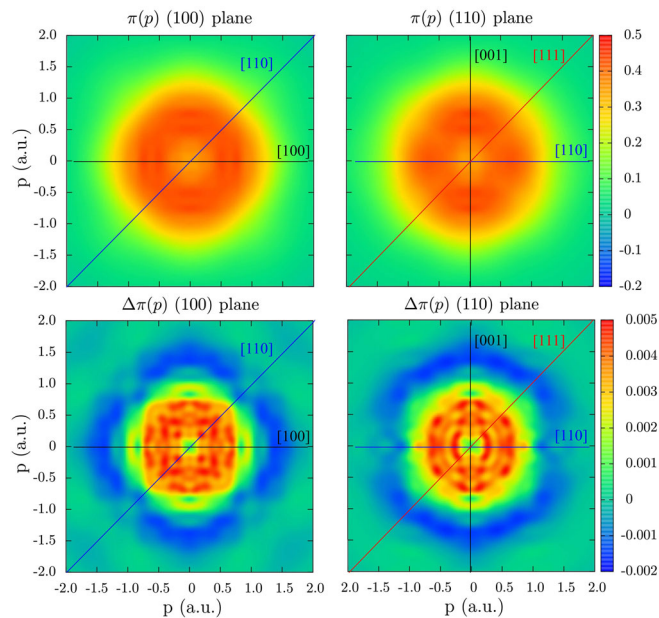


FIG. 4 (color online). 2D maps of the valence EMD of LiF in the (100) and (110) planes and the two corresponding thermal differences between 300 and 10 K, as computed with the PBE0 hybrid functional. High-symmetry directions are marked.

\*alessandro.erba@unito.it

- [1] R. R. Zope, *Phys. Rev. A* **62**, 064501 (2000).
- [2] *X-ray Compton Scattering*, edited by M. J. Cooper, P. E. Mijnarends, N. Shiotani, N. Sakai, and A. Bansil (Oxford University Press, Oxford, 2004).
- [3] Y. Sakurai, M. Itou, B. Barbiellini, P. E. Mijnarends, R. S. Markiewicz, S. Kaprzyk, J.-M. Gillet, S. Wakimoto, M. Fujita, S. Basak *et al.*, *Science* **332**, 698 (2011).
- [4] J. T. Okada, P. H. -L. Sit, Y. Watanabe, Y. J. Wang, B. Barbiellini, T. Ishikawa, M. Itou, Y. Sakurai, A. Bansil, R. Ishikawa *et al.*, *Phys. Rev. Lett.* **108**, 067402 (2012).
- [5] J. R. Hart and A. J. Thakkar, *Int. J. Quantum Chem.* **102**, 673 (2005).
- [6] A. J. Thakkar, *Adv. Chem. Phys.* **128**, 303 (2004).
- [7] A. Erba, C. Pisani, S. Casassa, L. Maschio, M. Schütz, and D. Usvyat, *Phys. Rev. B* **81**, 165108 (2010).
- [8] A. Erba, M. Itou, Y. Sakurai, R. Yamaki, M. Ito, S. Casassa, L. Maschio, A. Terentjev, and C. Pisani, *Phys. Rev. B* **83**, 125208 (2011).
- [9] C. Pisani, M. Itou, Y. Sakurai, R. Yamaki, M. Ito, A. Erba, and L. Maschio, *Phys. Chem. Chem. Phys.* **13**, 933 (2011).
- [10] C. Pisani, A. Erba, S. Casassa, M. Itou, and Y. Sakurai, *Phys. Rev. B* **84**, 245102 (2011).
- [11] C. Pisani, A. Erba, M. Ferrabone, and R. Dovesi, *J. Chem. Phys.* **137**, 044114 (2012).

- [12] T. S. Koritsanszky and P. Coppens, *Chem. Rev.* **101**, 1583 (2001).
- [13] K. Nygård, M. Hakala, S. Manninen, M. Itou, Y. Sakurai, and K. Hämäläinen, *Phys. Rev. Lett.* **99**, 197401 (2007).
- [14] M. J. Cooper, E. Zukowski, D. N. Timms, R. Armstrong, F. Itoh, Y. Tanaka, M. Ito, H. Kawata, and R. Bateson, *Phys. Rev. Lett.* **71**, 1095 (1993).
- [15] A. Dashora, B. L. Ahuja, A. Vinesh, N. Lakshmi, M. Itou, and Y. Sakurai, *J. Appl. Phys.* **110**, 013920 (2011).
- [16] P. K. Lawson, J. E. McCarthy, M. J. Cooper, E. Zukowski, D. N. Timms, F. Itoh, H. Sakurai, Y. Yanaka, H. Kawata, and M. Ito, *J. Phys. Condens. Matter* **7**, 389 (1995).
- [17] A. Koizumi, G. Motoyama, Y. Kubo, T. Tanaka, M. Itou, and Y. Sakurai, *Phys. Rev. Lett.* **106**, 136401 (2011).
- [18] B. L. Ahuja, A. Dashora, H. S. Mund, K. R. Priolkar, S. M. Yusuf, M. Itou, and Y. Sakurai, *Europhys. Lett.* **107**, 27005 (2014).
- [19] B. Ahuja, H. Mund, J. Sahariya, A. Dashora, M. Halder, S. Yusuf, M. Itou, and Y. Sakurai, *J. Alloys Compd.* **633**, 430 (2015).
- [20] S. B. Dugdale and T. Jarlborg, *Solid State Commun.* **105**, 283 (1998).
- [21] K. Chen, V. Caspar, C. Bellin, and G. Loupiau, *Solid State Commun.* **110**, 357 (1999).
- [22] C. Sternemann, G. Döring, C. Wittkop, W. Schülke, A. Shukla, T. Buslaps, and P. Suortti, *J. Phys. Chem. Solids* **61**, 379 (2000).
- [23] C. Sternemann, T. Buslaps, A. Shukla, P. Suortti, G. Döring, and W. Schülke, *Phys. Rev. B* **63**, 094301 (2001).
- [24] S. Huotari, K. Hämäläinen, S. Manninen, C. Sternemann, A. Kaprolat, W. Schülke, and T. Buslaps, *Phys. Rev. B* **66**, 085104 (2002).
- [25] R. Dovesi, R. Orlando, A. Erba, C. M. Zicovich-Wilson, B. Civalleri, S. Casassa, L. Maschio, M. Ferrabone, M. De La Pierre, Ph. D'Arco *et al.*, *Int. J. Quantum Chem.* **114**, 1287 (2014).
- [26] M. F. Peintinger, D. V. Oliveira, and T. Bredow, *J. Comput. Chem.* **34**, 451 (2013).
- [27] W. A. Reed, P. Eisenberger, F. Martino, and K. F. Berggren, *Phys. Rev. Lett.* **35**, 114 (1975).
- [28] K. F. Berggren, F. Martino, P. Eisenberger, and W. A. Reed, *Phys. Rev. B* **13**, 2292 (1976).
- [29] G. Loupiau and J. Petiau, *J. Phys. II (France)* **41**, 265 (1980).
- [30] J. P. Perdew and K. Schmidt, *AIP Conf. Proc.* **577**, 1 (2001).
- [31] N. W. Ashcroft and N. D. Mermin, *Solid State Physics* (Saunders College, Philadelphia, 1976).
- [32] S. Baroni, P. Giannozzi, and E. Isaev, *Rev. Mineral. Geochem.* **71**, 39 (2010).
- [33] R. E. Allen and F. W. De Wette, *Phys. Rev.* **179**, 873 (1969).
- [34] A. Erba, *J. Chem. Phys.* **141**, 124115 (2014).
- [35] A. Erba, M. Shahrokhi, R. Moradian, and R. Dovesi, *J. Chem. Phys.* **142**, 044114 (2015).
- [36] B. Yates and C. H. Panter, *Proc. Phys. Soc.* **80**, 373 (1962).
- [37] M. E. Straumanis and J. S. Shah, *Z. Anorg. Allg. Chem.* **391**, 79 (1972).
- [38] A. Erba, J. Maul, R. Demichelis, and R. Dovesi, *Phys. Chem. Chem. Phys.* **17**, 11670 (2015).
- [39] A. Erba, J. Maul, M. De La Pierre, and R. Dovesi, *J. Chem. Phys.* **142**, 204502 (2015).
- [40] A. Erba and C. Pisani, *J. Comput. Chem.* **33**, 822 (2012).